Biomech Model Mechanobiol (2011) 10:133–145
DOI 10.1007/s10237-010-0222-x

ORIGINAL PAPER

Multiscale methodology for bone remodelling simulation using coupled finite element and neural network computation

Ridha Hambli · Houda Katerchi · Claude-Laurent Benhamou

Received: 7 October 2009 / Accepted: 3 May 2010 / Published online: 27 May 2010

Abstract The aim of this paper is to develop a multiscale hierarchical hybrid model based on finite element analysis and neural network computation to link mesoscopic scale (trabecular network level) and macroscopic (whole bone level) to simulate the process of bone remodelling. As whole bone simulation, including the 3D reconstruction of trabecular level bone, is time consuming, finite element calculation is only performed at the macroscopic level, whilst trained neural networks are employed as numerical substitutes for the finite element code needed for the mesoscale prediction. The bone mechanical properties are updated at the macroscopic scale depending on the morphological and mechanical adaptation at the mesoscopic scale computed by the trained neural network. The digital image-based modelling technique using μ-CT and voxel finite element analysis is used to capture volume elements representative of 2 mm^3 at the mesoscale level of the femoral head. The input data for the artificial neural network are a set of bone material parameters, boundary conditions and the applied stress. The output data are the updated bone properties and some trabecular bone factors. The current approach is the first model, to our knowledge, that incorporates both finite element analysis and neural network computation to rapidly simulate multilevel bone adaptation.

R. Hambli (✉)
Institut Prisme, MMH, 8, rue Léonard de Vinci,
45072 Orléans cedex 2, France
e-mail: ridha.hambli@univ-orleans.fr

H. Katerchi
LGM-ENIM, Avenue Ibn El Jazzar, 5019 Monastir, Tunisia

C.-L. Benhamou
CHR d'Orléans, IPROS, Inserm U658, 1 rue Porte Madeleine,
45032 Orléans Cedex 1, France

Keywords Bone remodelling · Multiscale · Hierarchical · Finite element · Neural network

1 Introduction

Bone is a hierarchically organized material. Its adaptation strongly depends on its trabecular structure which can be assessed by changes to its morphological and mechanical properties over time (Tovar 2004; Yoo and Jasiuk 2006).

In 2004, Poter proposed an analytical scheme for multiscale modelling of bone as a natural hybrid nanocomposite to predict the individual properties of the component materials. The proposed model gives a good estimation of Young's modulus of cortical bone compared with the available experimental data, although it is not able to provide data regarding stress distribution and evolution of bone microstructure. Sansalone et al. (2007) used a 2D multiscale modelling method to investigate the mechanical properties of bone. Their procedure provides the mechanical response at a given scale. Ghanbari and Naghdabadi (2009) have used a hierarchical multiscale modelling scheme for the analysis of cortical bone, considering it a nanocomposite. Two boundary value problems were defined, one for macroscale and another for microscale. The coupling between these scales is done by using the homogenization technique. Despite the progress in the field of bone multiscale modelling, there remains a lack of models integrating bone structural information at different scales and the remodelling process (Viceconti et al. 2008). Computational models of the bone remodelling process must address the changes in bone structure on multiple levels, allowing for a more accurate description of the whole bone (Adachi et al. 1999; Fernandes et al. 1999; Bagge 2000; Huiskes et al. 2000; McNamara and Prendergast 2007; Hambli et al. 2009). This process occurs at different time and spatial scales in

a hierarchical way with interacting phenomena linking the different scales (Weiner and Traub 1992; Rho et al. 1998; Tovar 2004; Yoo and Jasiuk 2006). In recent years, a number of mathematical models have been proposed to explain and simulate the remodelling process. Whilst these models provide valuable insights, so far they only address changes in bone structure/properties using homogenization methods based on idealized 2D or 3D trabecular structures (Adachi et al. 1998, 1999; Yoo and Jasiuk 2006; Fernandes et al. 1999; Bagge 2000; Jacobs 2000; Sansalone et al. 2007). Furthermore, among the various multiscale modelling approaches, hierarchical multiscale modelling methods are more advantageous than homogenization methods for determining the interactions of the various levels.

Recently, Leardini et al. (2006), Viceconti et al. (2007, 2008) have has developed an anatomo-functional multiscale supermodel of the human musculoskeletal system that is able to predict the risk of bone fracture under routinely conventional physical loads. They incorporated a stochastic constitutive law to represent the variation of bone material responses with respect to position and time. The proposed supermodel is conceived as the interconnections of five interdependent sub-models: the continuum, the boundary conditions, the constitutive equations, the remodelling history and the failure criterion. The entire anatomo-functional supermodel is defined as a collection of procedural macros able to predict the risk of fracture for the subject specific. Application of this model is complex due to its basis on serial executions of the sub-models. Moreover, integration of the various sub-models into a single phase execution was not proposed, rendering its application for daily clinical usage lengthy and time consuming. Jang and Kim (2010) developed a numerical framework that computationally determines simultaneous and interactive structural changes of the cortical and trabecular bone types during bone remodelling. A 2D micro-finite element (μFE) model was constructed which represents the entire cortical bone and total trabecular architecture in human proximal femurs. One limitation of their study is that it considers 2D adaptation at the meso level, thus leaving it unable to capture the realistic 3D nature of the bone remodelling process.

In the present paper, we describe a rapid multiscale approach for a simulation of the bone remodelling process, using 2D finite element (FE) analysis at the macro level and 3D neural network (NN) computation at the meso level. We distinguish between the following structural levels: macrostructure (whole bone) and mesostructure (trabecular architecture).

From a numerical point of view, the tissue (macro) scale transfers information to the mesoscale in the form of macroscopic variables and boundary conditions obtained at each FE of the mesh after solving the macroscopic analysis using FEM. At the mesoscopic scale, the local boundary conditions (derived from the macro FE results) are applied to the mesoscopic bone model, and trained NN allow for the computation of the meso model responses. Finally, the mesoscale transfers information back to the macroscale in the form of averaged updated material properties.

The digital image-based modelling technique, using μ-CT and voxel finite element analysis, is used to capture representative volume elements (RVE) of 2 mm^3 at the mesoscale level in the femoral head. The input data for the artificial neural network are a set of bone material parameters, boundary conditions and the applied stress. The output data are the updated bone properties and some trabecular bone factors. The NN approach is beneficial if the numerical analysis of the complex model is time consuming or unfeasible (Topping and Bahreininejad 1992; Jenkins 1997; Rafiq et al. 2001; Unger and Konke 2008; Hambli et al. 2006). Moreover, NN models can be applied for the integration of information extracted from experimental data and medical images. Another advantage of the method is that the linking phase between the different scales and the application of an inverse calculation can be performed easily and rapidly (Jenkins 1997; Rafiq et al. 2001).

2 Method

The proposed 'hybrid FE and neural network' (FENN) method is a simulation procedure in which a continuum model of bone is discretized into smaller sub-models. A trained NN is applied locally to determine any structural and mechanical changes in the trabecular network. The local results are then passed back to the global level model. Changes in the material distribution of the continuum model will have an effect on the stress and strain fields' distribution, thus affecting the mechanical stimulus of each meso model in the subsequent iteration. A schematic illustration of the FENN approach is presented in Fig. 1.

In the current study, investigations into the mesoscale are based on computed microtomography scans of 2 mm^3 uniform RVE specimens acquired at 40 μm voxel sizes (Fig. 2).

The meso approach can be summarized by the five following steps:

(i) FE remodelling simulations of the RVE for different combinations of bone inputs.
(ii) Averaging the RVE outputs.
(iii) Steps (i) and (ii) supply training data in the form of a 'design of experiments' (DoE) table for NN training.
(iv) Training the NN based on the numerical DoE.
(v) Incorporation of the NN into the macro FE model to link meso-to-macro scales.

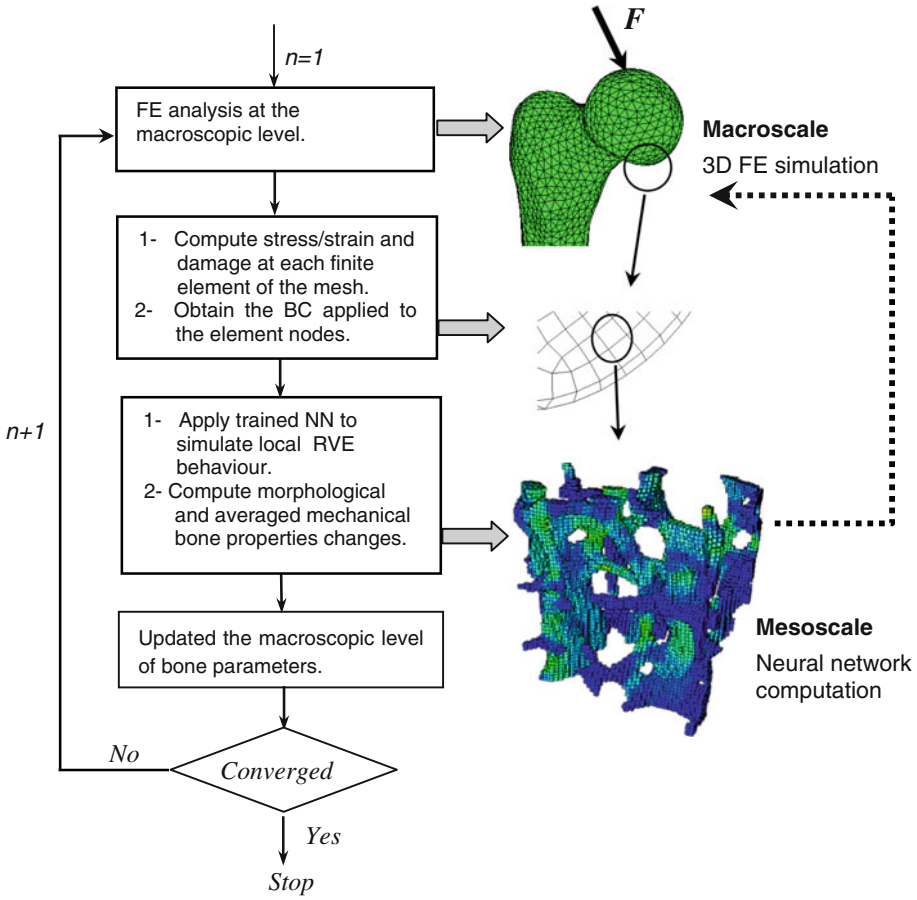

Fig. 1 Multiscale FENN approach for bone analysis: Two-level analysis for predicting the remodelling process. *Macroscale level*: whole bone computed using FE analysis. *Mesoscale level*: computed using trained NN

In the following subsections, each item (i)–(v) of the mesomodel is explained in detail.

2.1 Finite element model for the macroscale

There are three different materials in the model; trabecular bone, cortical bone and marrow. However, the mechanical influence of the marrow component is negligible with respect to the bone matrix (Martínez-Reina et al. 2009).

Structurally, bone tissue is a composite material with a complex hierarchical structure. At the continuum level, the effective properties of bone depend on its structure and, hence, exhibit anisotropic behaviour. In cortical bone, porosity is very low and anisotropy is mainly controlled by the lamellar and osteonal orientations. In trabecular bone, porosity is higher and the major determinant of anisotropy is the trabecular orientation. Anisotropic behavioural laws have been proposed by several authors to simulate bone behaviour (Jacobs et al. 1997; Hart and Fritton 1997; Fernandes et al. 1999; Doblare and Garcia 2002; Martínez-Reina et al. 2009). As the investigation scale of the present work corresponds to the macro level, we have considered, for simplicity, averaged isotropic bone behaviour (Tovar 2004). In a future work, the proposed model should be extended to include anisotropy and marrow influences.

The behaviour law for cortical and cancellous bone at the macro level is expressed as:

$$\sigma_{ij} = a_{ijkl}\varepsilon_{kl} \tag{1}$$

σ_{ij} is the stress, ε_{kl} is the strain and a_{ijkl} is the isotropic elasticity stiffness tensor.

Damage is not considered at the macro level, its coupling effects are introduced in the mesoscopic formulation at the trabecular level. Furthermore, remodelling of cortical bone is not considered in this primary study. Nevertheless, the macroscopic FE model can be extended to describe remodelling process for both cortical and cancellous bone.

2.2 Finite element model of the mesoscale for NN training

The effective properties of trabecular bone are modelled as elastic isotropic behaviour coupled with damage incorporating strain and microdamage stimulus (McNamara and Prendergast 2007).

The behaviour law is expressed by:

$$\sigma_{ij} = (1 - D)a_{ijkl}\varepsilon_{kl} \tag{2}$$

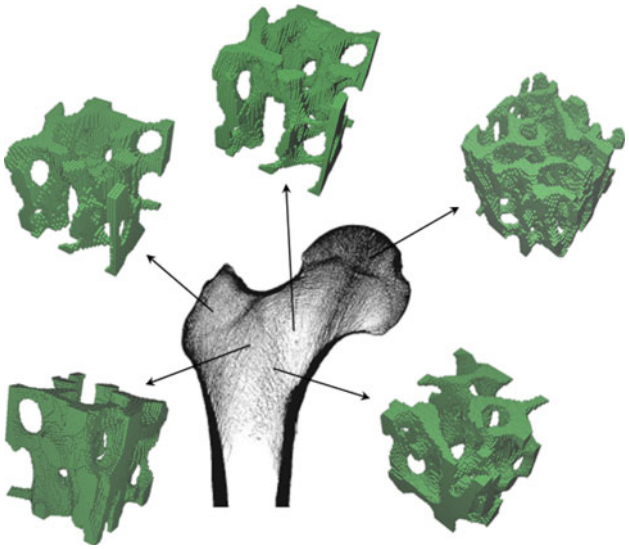

Fig. 2 Five representative volume elements (*RVE*) obtained using a digital image-based modelling technique using μ-CT and voxel FE mesh (40 μm) at five different bone zones. Each RVE consists of 2 mm^3 trabeculae network meshed using eight nodes brik elements

σ_{ij} is stress, D is the damage variable, ε_{kl} is strain and a_{ijkl} is the isotropic elasticity stiffness tensor.

For high cycle fatigue under purely elastic strain, without coupling between the heat dissipation and mechanical dissipation, Chaboche (1981) proposed a non linear damage model given by:

$$D = 1 - \left[1 - \left(\frac{N}{N_f}\right)^{\frac{1}{1-\alpha}}\right]^{\frac{1}{1+\beta}} \tag{3}$$

where α and β are material parameters and N_f is the cycle at failure which can be obtained as described by Martin et al. (1998):

$$N_f^c = 1.479 \times 10^{-21} \Delta\varepsilon^{-10.3} \quad \text{for compressive loads} \tag{4a}$$

$$N_f^t = 3.630 \times 10^{-32} \Delta\varepsilon^{-14.1} \quad \text{for tensile loads} \tag{4b}$$

where $\Delta\varepsilon$ is the amplitude of the applied microstrain.

The set of equation describing the fully coupled change in the bone density is given by (Hambli et al. 2009):

$$\frac{\mathrm{d}\rho}{\mathrm{d}t} = \alpha_R (S - S_R) \quad \text{If} \quad S < S_R \tag{5a}$$

$$\frac{\mathrm{d}\rho}{\mathrm{d}t} = 0 \quad \text{If} \quad S_R \leq S \leq S_F \tag{5b}$$

$$\frac{\mathrm{d}\rho}{\mathrm{d}t} = \alpha_F (S - S_F) \quad \text{If} \quad S_F < S < S_D \tag{5c}$$

$$\frac{\mathrm{d}\rho}{\mathrm{d}t} = \alpha_D (S - S_D) \quad \text{If} \quad S \geq S_D \tag{5d}$$

where ρ is the bone density, t is time and S is the coupled strain-damage stimulus function. α_R, α_F and α_D denote respectively bone resorption rate, bone formation rate and damage resorption rate.

S_R, S_F and S_D denote respectively target levels of strain-damage energy density for bone resorption, formation and damage resorption.

The stimulus can be expressed by (Mullender and Huiskes 1995):

$$S(x,\ t) = \sum_{i=1}^{N_{oc}} f_i(x) \mu_i\ S_i \tag{6}$$

where μ_i is the mechanosensitivity of the osteocyte i and N_{oc} is the number of osteocytes. $f_i(x)$ is a spatial influence function defined by (Mullender and Huiskes 1995):

$$f_i(x) = \exp(-d_i(x)/d_0) \tag{7}$$

where $d_i(x)$ is the distance between the osteocyte i and the bone surface location x. The parameter d_0 represents a normalization factor limiting the influence area of the osteocyte.

S_i is the local stimulus value expressed in terms of coupled strain-damage energy density and is expressed by (Hambli et al. 2009):

$$S = \frac{1}{2} \frac{(1 - D)\, \sigma_{ij}\ \varepsilon_{ij}}{\rho} \tag{8}$$

The new density value of the bone tissue is approximated using forward Euler method by:

$$\rho_{t+\Delta t}^i = \rho_t^i + \Delta\rho^i \tag{9}$$

The elastic modulus E at each location is expressed by (Hambli et al. 2009):

$$E = C\,(1 - D)\,\rho^{\gamma} \tag{10}$$

where C and γ are experimentally derived constants.

The averaging relation of each RVE outputs, y_i^{RVE}, is expressed by (Ghanbari and Naghdabadi 2009):

$$y_i^{\mathrm{RVE}} = \frac{1}{V_o} \int_{V_O} y_i \mathrm{d}V \tag{11}$$

where V_o and y_i denote respectively the RVE reference domain and the output at every finite element location i.

2.3 Design of experiments preparation for NN training

According to the proposed FENN method described in Sect. 2, the micro-tomography and the FE simulations as well as the averaging of the RVE (points i and ii) supply training data for NN (step iii).

Table 1 Selected inputs and outputs for NN training

Inputs	Level	Values				
Frequency (cycle/day)	4	$1.e^3$	$4.e^3$	$7.e^3$	$10.e^3$	–
Applied stress (MPa)	5	0	30	60	100	150
Stress orientation (°)	5	−45	−22.5	0	22.5	45

Outputs	Description
Average density	ρ
Average damage	D
Average elastic modulus	E
Average stimulus	S

The inputs applied to the RVEs are used to generate the design of experiments for the NN training (steps (i) of the meso approach described in Sect. 2). The outputs are FE-averaged responses of the RVEs corresponding to the inputs (step ii)

To prepare the training patterns and data for the NN, the analysis was divided into two separate problems; (a) Macroscale FE analyses were performed to determine the boundary conditions (stress amplitude and orientation) applied at every FE of the mesh during one-legged stance for different loadings, orientations and frequencies, and (b) The results of the macroscale FE analysis were used to define the local applied boundary conditions on the μ-CT voxel finite element. The retained inputs for the NN training are the amplitude of the applied stress, the stress orientation as it depends on the bone site location and the load frequency depending on the daily activities. The outputs are the average bone density (ρ), the average damage (D), the average elastic modulus (E) and the averaged stimulus (S). This set of outputs represents one of the main variables used by the clinicians to assess bone quality (Keyak et al. 2001 and Bessho et al. 2007). Other inputs/outputs can influence the remodelling response. The aim of the current primary work is to implement the FENN method and to check its validity for rapid multiscale prediction of the remodelling process. The FE model for NN training can be extended by including more bone material variables and inputs in order to capture complex bone behaviour. Three main inputs have been retained here with four to five levels for each factor (Table 1). Full factorial combinations of the inputs produced 100 ($4 \times 5 \times 5$) factorial experimental designs to study the effect of each input (Fig. 3).

100 μ-CT FE simulations were performed corresponding to the combinations of the selected inputs for RVE bone remodelling. The cumulative computation time was about 27 h on a 2 Giga dual-core computer.

2.4 Neural network modelling

A NN model is a parallel processing architecture consisting of a large number of inter-connected processing elements

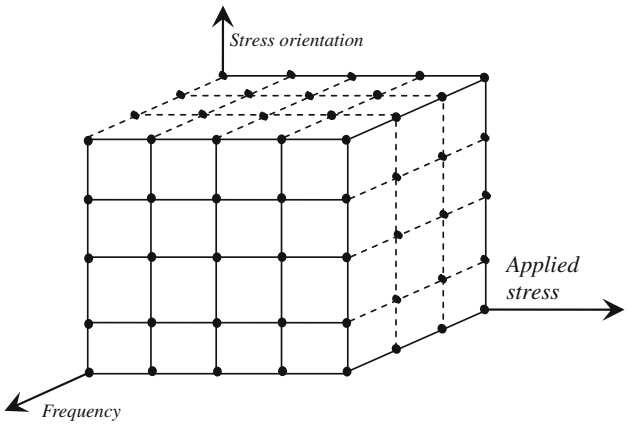

Fig. 3 The NN training patterns based on full combinations of the selected input factors

called neurons organized in layers. A NN model can be used for the mapping of input to output data without a known 'a priori' a relationship between those data. NNs have been widely and increasingly employed in the analysis of problems in science and technology (Topping and Bahreininejad 1992; Jenkins 1997; Rafiq et al. 2001; Hambli et al. 2006). One of the distinct characteristics of the NN is its ability to learn and generalize from experience and examples and to adapt to changing situations following an initial training phase. NNs are able to map causal models (i.e. mapping from cause to effect for estimation and prediction) and inverse mapping (i.e. mapping from effect to possible cause) (Jenkins 1997).

The training process in the NN involves presenting a set of examples (input patterns) with known outputs (target output). The system adjusts the weights of the internal connections to minimize errors between the network output and target output. The knowledge is represented and stored by the strength (weights) of the connections between the neurones (Topping and Bahreininejad 1992; Jenkins 1997; Rafiq et al. 2001; Hambli et al. 2006).

After the NN is satisfactorily trained and tested, it is able to generalize rules and respond to input data in order to predict required output rapidly (seconds) within the domain covered by the training examples (Topping and Bahreininejad 1992; Jenkins 1997; Rafiq et al. 2001; Hambli et al. 2006).

A single neuron performs a weighted sum of the inputs x_i that are generally the outputs of the neurons of the previous layer v_m, adding threshold value b_i and producing an output given by:

$$v_m = \sum_{i=1}^{L} w_{im} x_i + b_i \tag{12}$$

where w_{im} are the network weights.

Input signals accumulated in the neuron block are activated by either a linear or nonlinear function to generate

approximated NN output y_m given by:

$$y_m = f(v_m) \tag{13}$$

Amongst the activation functions, the sigmoid (logistic) function is the most commonly employed in NN applications. It is given by:

$$f(v_m) = \frac{1}{1 + \exp(-\beta v_m)} \tag{14}$$

where β is a parameter defining the slope of the function.

2.4.1 Neural network training

The training process in the NNs involves presenting a set of examples (input patterns) with known outputs (target output). The system adjusts the weights w_{lm} of the internal connections to minimize errors between the network output and target output. The knowledge is represented and stored by the strength (weights) of the connections between the processors.

There are several algorithms in a NN and the one used in the current analysis is the back-propagation (BP) training algorithm. The BP algorithm is an iterative gradient algorithm designed to compute the connection weights, minimizing the total mean square error between the actual output of the multilayer network and the desired output. In particular, the weights are initially chosen randomly and the rule consists of a comparison of the known and desired output value with the calculating output value by utilizing the current set of weights and threshold.

The learning algorithm can be summarized as follows:

Step 1. Select the learning rate η and momentum coefficient α

Step 2. Take a group of random numbers within $(-1, 1)$ as the initial values of the weights w_{jk}.

Step 3. Compute the outputs of all neurons, layer by layer, starting with the input layer using Eqs. 1–3

Step 4. Compute the system mean square error by:

$$E = \frac{1}{2}\frac{1}{P}\sum_{1}^{P}\sum_{i-1}^{N}(D_{im} - y_{im})^2 \tag{15}$$

where y_{im} is the actual output of the ith output node with regard to the mth training pattern, while D_{im} is the corresponding desired output

P and N denote respectively the total number of patterns and the number of output nodes,

Step 5. If E is small enough or the learning iteration is too high, stop learning.

Step 6. Compute the learning errors for every neuron layer by layer as follows:

$$\delta_m = (D_m - y_m)\ v_m \tag{16}$$

Step 7. Update the weights along the negative gradient of the error E:

$$w_{jk}(t+1)) = w_{jk}(t) + \eta\ \delta_k\ y_j + \alpha\ \left[w_{jk}(t) - w_{jk}(t-1)\right] \tag{17}$$

Step 8. Repeat by returning to Step 3.

In the present work, an in-house NN program called Neuromod written in Fortran (Hambli et al. 2006) has been developed and incorporated into Abaqus finite element code via the user routine UMAT to link the meso and the macro scales. Neuromod includes a module which allows for the automatic selection of the best architecture of the network and the best values of the learning rate η and momentum coefficient α based on the following steps:

- Select an initial configuration of the NN (typically, one hidden layer with the number of hidden units set to half the sum of the number of input and output units) and select initial values of the learning rate η and momentum coefficient α ($\eta = 0.01$ and $\alpha = 0.01$).
- Iteratively, conduct a number of calculations with each configuration, retaining the best network (in terms of verification error) found.
- For each calculation, if under-learning occurs (the network doesn't achieve an acceptable performance level) try adding more neurons to the hidden layer(s). If this is not effective, try adding an extra hidden layer. If over-learning occurs (verification error begins to rise) try removing hidden units (and possibly layers).

In the present work, the selected architecture is based on double hidden layers with five neurones per layer with a learning rate factor of $\alpha = 0.1$ and a momentum coefficient of $\eta = 0.1$.

In summary, the main steps to apply NN computation can be described by the following steps:

1. Build the architecture of the NN.
2. Prepare a design of the experimental table for NN training.
3. Train the NN.
4. Apply the trained NN for prediction: Execution time is several seconds.

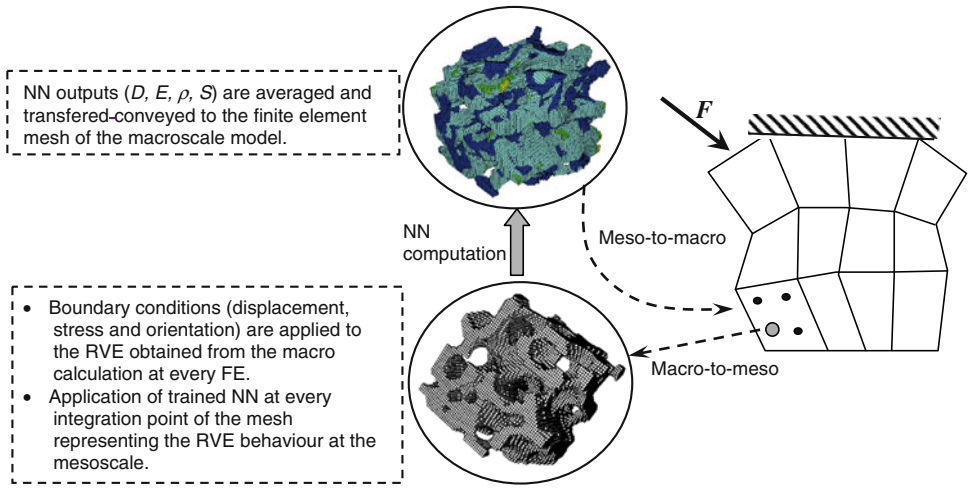

Fig. 4 Meso-to-macro transition: NN is incorporated into the FE code Abaqus via the routine UMAT. During the FE calculation at the macro level, the NN is called at every integration point to compute the averaged outputs representing the RVE behaviour at the meso scale

2.5 Meso-to-macro transition

The transition from the mesoscale to the macroscale is done by employing the trained NN. The mesoscale model (NN) able to predict detailed responses was incorporated into the macroscale model as a material formulation on the integration point level at every FE iteration—e.g. the behaviour law needed to compute the outputs at the mesoscale was substituted by the trained NN. Equation 11 was applied to average the RVE μ-CT and voxel FE outputs.

Figure 4 shows the meso-to-macro linking scheme incorporated into the Abaqus code via UMAT routine.

3 Simulation of multiscale femoral head remodelling

To illustrate the capabilities of the FENN method, remodelling of a 2D femur head was performed. A FE model was constructed including the proximal femur articulating freely with a representation of the acetubulum (Fig. 5).

A 2D mesh was generated using four-node stress plane elements at the macroscopic level. The same behavioural law and bone properties have been assigned to the cortical bone and acetubulum. The trained NN was applied at every integration point of the mesh to describe the 3D behaviour of the cancellous bone despite the 2D model being retained for the macro model. Although clinical observations provided valuable information regarding the changes of cortical and trabecular bone types during growth or ageing, little is known about how each of the cortical and trabecular bone types change and how they interact with one another during the bone remodelling process (Jang and Kim 2010). Thus, thresholding between cortical and cancellous bone is modelled by

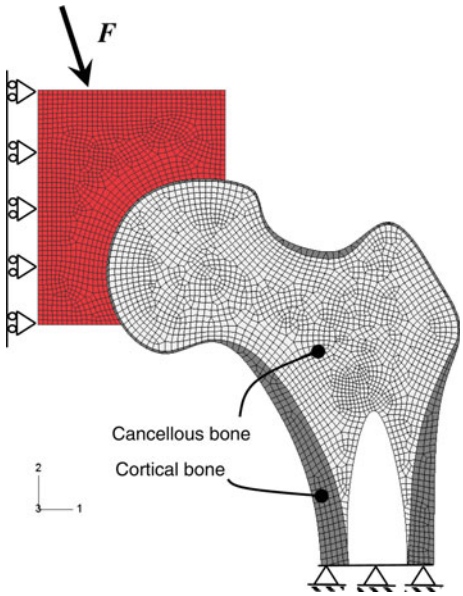

Fig. 5 FE of the whole femur and acetabulum. The model is fixed at the bottom and loaded through the acetabulum. Cortical bone (*dark grey*), cancellous bone (*light grey*) and acetabulum (*red*), marrow (*white*) are not considered here

two bone regions with different behaviour laws and material properties.

Contact between the femoral head and the acetubulum was modelled using contact elements with a zero friction value to ensure that only normal forces were transmitted.

The macro model is run in alternating maximum load ($F = 3{,}500$ N) and unload ($F = 0$ N) increments during 100 iterations (days) with a fixed number of cycles per day (7,000 cycles/day). The applied loading cycles on the acetubulum with an orientation of 24° from the vertical generate

Table 2 Material properties for bone used for the remodelling simulation from (McNamara and Prendergast 2007; Hambli 2009)

Parameters	Notation	Trabecular bone	Acetubulum and cortical bone
General parameters			
Initial elastic modulus	E_0 (MPa)	4,000	12,000
Poisson ratio	ν	0.3	0.3
Initial density	ρ (g/cm^3)	0.6	1.2
Density coefficient	C (g/cm^3)	4,000	–
Density exponent	γ	3	–
Damage law parameters			
Fatigue parameter	α	0.2	–
Fatigue exponent	β	0.4	–
Damage evolution parameters			
Time step size (iteration)	Δt (day)	1	1
Cycles per day	N (day)	5,000	5,000
Stimulus parameters			
Bone resorption rate	α_R	0.035	–
Bone formation rate	α_F	0.045	–
Bone damage resorption rate	α_D	0.035	–
Stimulus reference value for bone disuse resorption	S_R (J.m^{-3})	0.0025	–
Stimulus reference value for bone formation	S_F (J.m^{-3})	0.007	–
Stimulus reference value for bone damage resorption	S_D (J.m^{-3})	0.01	–

uniformly increasing/decreasing local microstrain in several bone sites exceeding 3,500 $\mu\varepsilon$.

This critical level (3,500 $\mu\varepsilon$) has been reported by McNamara and Prendergast (2007) as the threshold strain amplitude for damage accumulation in bone.

Material properties for bone used for the simulation are given in Table 2.

4 Results

Figure 6 shows the contours of von Mises equivalent stress in trabecular bone obtained by using the conventional FE calculation (a) and the proposed multiscale FENN approach (b). As the focus here is to assess the remodelling of cancellous bone only, acetubulum and cortical bone was removed (post-processing) from the figures for a better analysis of the trabecular bone.

Observations of both contours reveal very similar shapes allowing for insight into the capability of the FENN method to predict the remodelling process when compared to the conventional FE method. Neverthless, the FENN approach predicts higher values of stresses. This can be explained by the fact that the 3D structure of cancellous bone generates stress concentration around the connected trabeculae (Fig. 6c, d). McNamara et al. (2006) numerically analysed the distributions of stress and strain within four connected trabeculae. The analyses predicted that 30% of the tissue had a strain greater than 4,000 $\mu\varepsilon$ which exceeds the threshold strain level (3,500 $\mu\varepsilon$) for damage accumulation in bone. Since the proposed FENN model incorporates the modelling of the real 3D trabecular networks, stress concentration (Fig. 6d) due to the trabecular shapes and connections leads to more accurate predictions of stress distribution than compared to conventional FE models.

Figure 7 shows the contour of trabecular bone damage after 100 iterations obtained using the FENN approach.

Keyak et al. (2001) compared experimental fracture sites on radiographs of 18 specimens. They reported that the predicted fracture sites were located in the sub-capital region in all specimens. FENN results predicted localized damage in the femoral neck which is qualitatively in conformity with possible fracture sites in femur necks (Faulkner et al. 1993; Bessho et al. 2007). In general, clinically available methods of estimating bone strength and the risk of fracture of the femoral neck include bone densitometry or peripheral

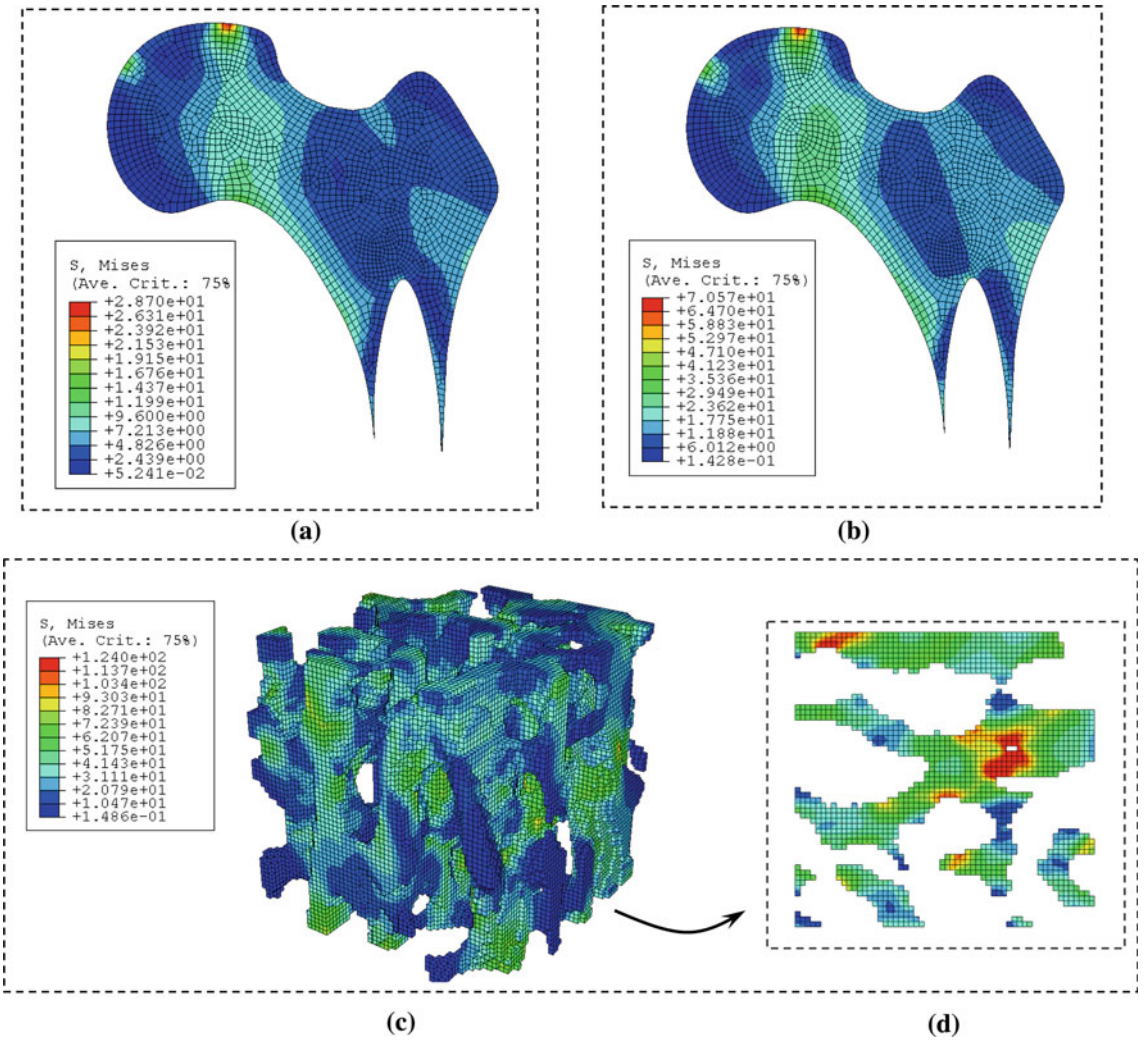

Fig. 6 Equivalent stress as predicted by FE and FENN methods. **a** Conventional FE. **b** FENN method. **c** RVE contour; **d** Stress concentration at a cross section

quantitative computed tomography and imaging procedures. These techniques evaluate regional bone density and morphology, which are partly related to fracture risk, but they are of limited value for quantifying structural strength (Faulkner et al. 1993). The FENN method, which incorporates information on the real 3D architecture and bone density distribution, could possibly achieve rapid non-invasive and precise clinical assessments of the strength of the proximal femur and possible sites of fracture (Bessho et al. 2007). Quantitative validation of the FENN model will be conducted in future work to compare predicted and observed in vivo remodelling activity.

In Fig. 8, the distribution of bone density is presented. The initial value was set to 0.6 g/cm^3. Noticeably, the results predicted by FENN model give a localized density adaptation in a region of high stresses.

In conventional FE simulation of trabecular bone, the apparent density variation based on averaged adaptation laws is frequently calculated. In the present work, the averaged apparent density is obtained explicitly from the averaged predicted NN computation on real RVE. Depending on the stimulus value, it is clear that regions with low stress intensity observed in Fig. 6b undergo density decreases and the regions with high stress values are subject to a density increase. We observed strong similarities in trabecular bone density contours between the FENN results and previously published finite element results (Stulpner et al. 1997; Hambli et al. 2009).

Figure 9 shows the evolution of average density of the whole bone versus iteration values. The FENN model leads to a steady increase in bone density as a consequence of the daily load amplitude and frequency. The RVE contour (Fig. 6c) predicts that very high stresses (>100 MPa) existed at the mesoscale. Therefore, bone density increases as a consequence of stress concentration effects. Stulpner et al. (1997) obtained similar results using a 3D finite element remod-

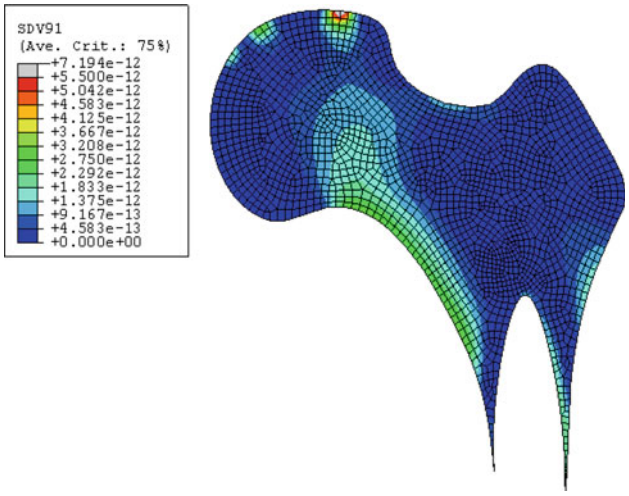

Fig. 7 Contour of trabecular bone damage as predicted by the FENN method

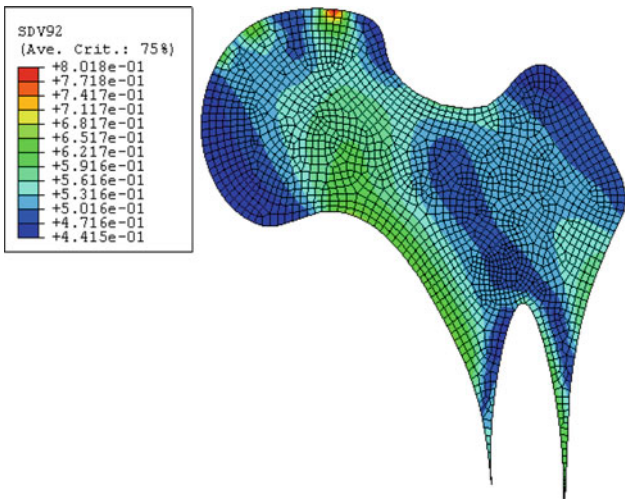

Fig. 8 Contour of trabecular bone density as predicted by the hybrid method

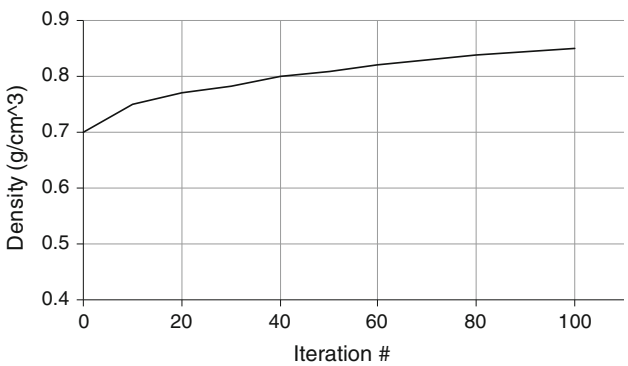

Fig. 9 Evolution of the average density of the whole bone as predicted by the FENN method

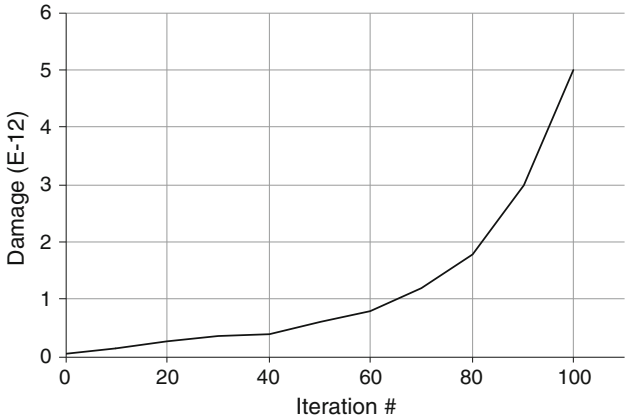

Fig. 10 Evolution of the average damage of the whole bone as predicted by the FENN method

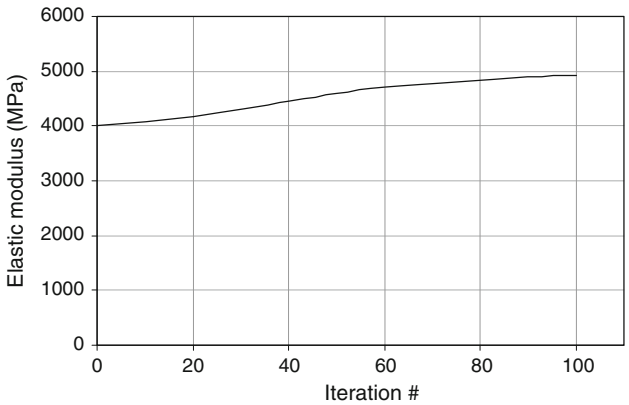

Fig. 11 Average Elastic modulus evolution of the whole bone

elling analysis of a femoral head adaptation. The authors predicted that a constant evolution of density occurred till iteration 1,000, and a steady state is reached after 300 iterations.

The average damage of the whole bone evolution versus iterations number is plotted in Fig. 10. We observed that the damage accumulation increases linearly from iteration 1 to iteration 60, followed by an increased rate of damage accumulation until iteration 100. This was due to the excessive load applied in the femoral head in some regions. The same trend was obtained by O'Brien et al. (2003) from experiments conducted on cortical bone.

The trabecular adaptation process may be explained in regard to bone stiffness. Bone stiffness is strongly related to the elastic modulus of bone. In this study, apparent bone elastic modulus, computed at the macro level, was assessed by the NN based on trabecular bone architecture, tissue modulus and bone volume fraction. Averaged elastic modulus evolution within the whole trabecular generated by the density variation is plotted in Fig. 11.

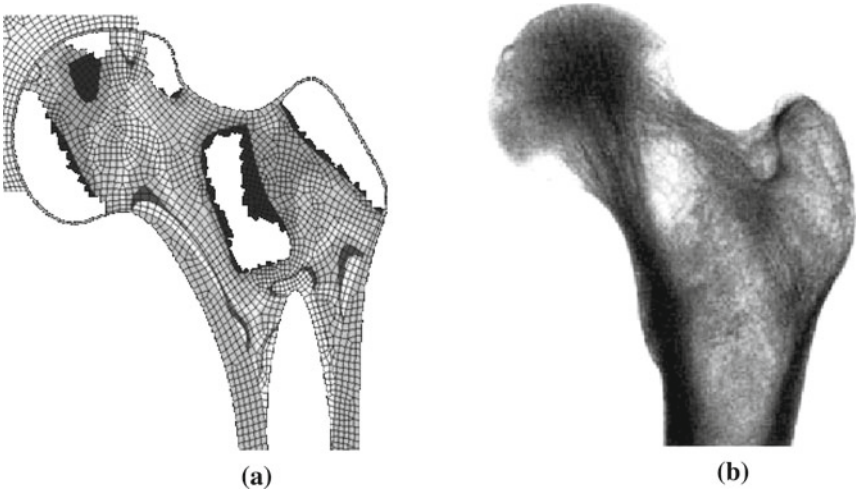

Fig. 12 Qualitative comparison between FENN predicted density distribution and a histological section of a proximal femur showing trabecular architecture. Figure adapted from Jacobs et al. (1997). **a** FENN predicted density distribution. **b** Histological section of a proximal femur. *White region* represents resorbed bone due to disuse

The observed increase in the average elastic modulus of the whole bone, from its initial value of 4,000 MPa, is a consequence of the average density increase and the damage accumulation obtained by Eq. 10. Continuum damage mechanics assumes that the damage model (Eq. 3) leads to a relative decrease in the elastic stiffness as the damage grows. Taylor et al. (2002) proposed a preliminary FE study to simulate the fatigue behaviour of cancellous bone. They examined the influence of material property degradation on the overall fatigue behaviour of a trabecular bone segment. In conclusion, their work suggested that the accumulation of damage plays an important role in reducing localized high stresses and redistributing the load to the surrounding tissue.

To illustrate the validity of the FENN method to predict trabecular adaptation on a proximal femur, the macro model is run in alternating load ($F = 2{,}000$ N) and unload ($F = 0$ N) increments for 300 iterations (days) with a fixed number of cycles per day (1,000 cycles/day) and an orientation of 24°. A qualitative comparative investigation was performed between the FENN results and radiography of the coronal section of a proximal femur (Fig. 12) adapted from (Jacobs et al. 1997).

Trabecular adaptation is generally considered to be a result of the changes to morphological properties of trabecular patterns: bone volume fraction, trabecular thickness, and structural anisotropy assessed by the NN computations. The NN outputs which incorporate such factors predict qualitatively similar femoral profiles as observed with the measured ones. It is well known that the shape of trabeculae is related to porosity and changes from slender rods to thick plates and vice versa. Moreover, trabecular orientation is influenced by mechanical load. Our model includes such factors in the 3D NN training phase. This allows for a better description of the architectural evolution of the cancellous bone which may affect the structural anisotropy of the proximal femur. The predicted results are based on referenced bone properties outlined in Table 2. Quantitative validation of the FENN model, however, is needed to compare predicted and observed in vivo remodelling activity.

Table 3 Computation times obtained by conventional FE and NN calculations

	FEM	NN
Computation time for one μ-CT RVE remodelling cycle (s)	970	1

As presented earlier, the proposed FENN model is able to rapidly predict multiscale trabecular bone remodelling. Table 3 gives details concerning the computation time of the mesoscopic responses for one remodelling cycle obtained by conventional FE (3D μ-CT for RVE) and NN computation (on RVE after training). A 2 Giga dual-core computer was used for the calculations.

Comparisons of data from Table 3 clearly show that the application of NN instead of conventional FE analysis is about 1,000 times faster. The rapidness of the FENN method highlights new perspectives concerning the multiscale analysis of biological tissues. Furthermore, NN approaches are beneficial for linking disparate dimensional scales, drastically reduce the computation time, incorporate the results of experimental and/or numerical calculations at low scales and to perform, if needed, inverse calculations to assess optimal inputs for given target outputs (Topping and Bahreininejad 1992; Jenkins 1997; Rafiq et al. 2001; Unger and Konke 2008; Hambli et al. 2006).

5 Discussion

During daily activities, bones are subjected to external forces which propagate through the trabecular network composed of 3D oriented interconnected trabeculae. Such 3D

structures generate stress concentrated around the connected trabeculae. The application of the FENN method leads to macro level averaged predictions, based on multiscale modelling from local 3D meso computations. Since the proposed FENN model incorporates the modelling of the real scanned trabeculae networks, we believe that taking into account stress concentration due to the trabeculae shapes and connections leads to a more accurate prediction of local and averaged results of the bone tissue as suggested by Cowin (2002). The author described a paradox in bone tissue which consists of the fact that the strains applied to whole bone (i.e., tissue level strains) are much smaller (0.04–0.3%) than the strains that are necessary to cause bone signalling in deformed cell cultures (1–10%).

In the current study, the focus was on the development and the implementation of a novel rapid multiscale approach for bone remodelling simulation using FE simulation at the macro level and 3D neural network computation at the meso level.

A finite element mesoscale model was developed to simulate the remodelling of a μ-CT 3D RVE trabecular bone. By averaging some selected mesoscopic outputs on RVE (density, damage, elastic modulus and stimulus), a macroscopic adaptation of trabecular bone was obtained from the mesoscale computations. The neural network is used to approximate this in relation to a macroscale simulation and replaces the material formulation of the cancellous bone, thus avoiding the computationally expensive parallel simulation on different scales.

Five current issues were addressed: (i) Simulation of the remodelling of RVE trabecular bone. (ii) Preparing a data base for the NN training. (iii) Training the NN to substitute the FE at the meso level by the NN. (iv) Linking meso-to-macro scales. (v) Application of trained NN for meso prediction. After a training phase, the NN algorithm was incorporated into a FE code to link the meso and macro scales and provide local and rapid computation at the meso scale.

In general, the hierarchical combination of trained NN models for the analysis of micro/mesoscales and FE macroscale models for bone modelling can be applied integrating information extracted from local FEM information, experiments and medical images into a global framework (such as electronic patient records or anatomo-functional databases). It should be noted that the proposed multiscale approach does not take into account all possible factors which may influence modelling/remodelling, including relevant biological mechanisms. The aim was to provide a framework using FE and NN methodology for a rapid and accurate prediction of multiscale modeling of bone. The FENN model can be extended by including multiscale cortical bone remodelling, additional bone material variables and inputs to capture complex bone behaviour.

Currently, there is a growing interest within the biomedical community, particularly from those with an interest in the human musculoskeletal system, in developing predictive multiscale methods capable of describing the mechano-biological processes occurring within the bone on different levels. The aim is to develop accurate prediction methods for the fracture risk of a specific patient (Viceconti et al. 2006). NN approaches are beneficial (i) to link disparate dimensional scales, (ii) to drastically reduce the computation time, (iii) to apply 3D local computations to capture the 3D bone adaptation effects, (iv) to incorporate results of experimental and/or numerical calculations at low scales and to (v) to perform inverse calculations to assess optimal inputs for given target outputs. In addition, NN models are very cost-effective when used for performing reliability analyses based on Monte Carlo simulations for biological tissue (Jenkins 1997; Hambli 2009).

We believe that the FENN analysis is a promising tool for assessing bone health and can be used in the clinical setting to evaluate the fracture risk for a specific subject. Moreover, a new generation of diagnostic instruments for osteoporosis can be equipped with trained NNs based on numerical prediction and/or population-specific referencing could yield precise and reliable results.

The current approach is, to our knowledge, the first model incorporating both FE analysis and NN computation to rapidly simulate the multilevel bone adaptation. We aim to further develop these computer simulations by including the increasingly sophisticated remodelling models such as micro and nano scales, anisotropic behaviour and bone cell activities.

It will be useful to address the limitations and challenges of this investigation in the future. Due to the restricted amount of clinical data, it was very difficult to directly compare our numerical results to in vivo experimental results from data sourced from the literature.

Acknowledgments The authors acknowledge the financial support provided by Agence Nationale de la Recherche (MoDos Project, ANR-09-TECS-018-04).

References

Adachi T, Tomita Y, Tanaka M (1998) Computational simulation of deformation behavior of 2D-lattice continuum. Int J Mech Solids 40:857–866

Adachi T, Tomita Y, Tanaka M (1999) Three-dimensional lattice continuum model of cancellous cone for structural and remodeling simulation. JSME Int J Ser C 42:470–480

Bagge M (2000) A model of bone adaptation as an optimization process. J Biomech 33:1349–1357

Bessho M, Ohnishi I, Matsuyama J, Matsumoto T, Imai K, Nakamura K (2007) Prediction of strength and strain of the proximal femur by a CT-based finite element method. J Biomech 40:1745–1753

Chaboche JL (1981) Continuum damage mechanics-a tool to describe phenomena before crack initiation. Nucl Eng Des 64:233–247

Cowin (2002) Mechanosensation and fluid transport in living bone. J Musculoskelet Neuronal Interact 2(3):256–260

Doblare M, Garcia JM (2002) Anisotropic bone remodelling model based on a continuum damage-repair theory. J Biomech 35(1): 1–17

Faulkner KG, Cummings SR, Black D, Palermo L, Gluer CC, Genant HK (1993) Simple measurement of femoral geometry predicts hip fracture: the study of osteoporotic fractures. J Bone Miner Res 8:1211–1217, 21:101–108

Fernandes P, Rodrigues H, Jacobs C (1999) A model of bone adaptation using a global optimisation criterion based on the trajectorial theory of Wolff. Comput Methods Biomech Biomed Eng 2(2):125–138

Ghanbari J, Naghdabadi R (2009) Nonlinear hierarchical multiscale modeling of cortical bone considering its nanoscale microstructure. J Biomech 42:1560–1565

Hambli R (2009) Statistical damage analysis of extrusion processes using finite element method and neural networks simulation. Finite Elem Anal Des 45(10):640–649

Hambli R, Chamekh A, BelHadj Salah H (2006) Real-time deformation of structure using finite element and neural networks in virtual reality applications. Finite Elem Anal Des 42(11):985–991

Hambli R, Soulat D, Gasser A, Benhamou CL (2009) Strain-damage coupled algorithm for cancellous bone mechano-regulation with spatial function influence. Comput Methods Appl Mech Eng 198(33–36,1):2673–2682

Hart RT, Fritton SP (1997) Introduction to finite element based simulation of functional adaptation of cancellous bone. Forma 12:277–299

Huiskes R, Ruimerman R, van Lenthe GH, Janssen JD (2000) Effects of mechanical forces on maintenance and adaptation of form in trabecular bone. Nature 405:704–706

Jacobs CR (2000) The mechanobiology of cancellous bone structural adaptation. J Rehabil Res Dev 37(2):209–216

Jacobs CR, Simo JC, Beaupre GS, Carter DR (1997) Adaptive bone remodeling incorporating simultaneous density and anisotropy considerations. J Biomech 30(6):603–613

Jang IG, Kim IY (2010) Computational simulation of simultaneous cortical and trabecular bone change in human proximal femur during bone remodeling. J Biomech 43:294–301

Jenkins WM (1997) An introduction to neural computing for the structural engineer. Struct Eng 75(3):38–41

Keyak JH, Rossi SA, Jones KA, Les CM, Skinner HB (2001) Prediction of fracture location in the proximal femur using finite element models. Med Eng Phys 23:657–664

Leardini A, Belvedere C, Astolfi L, Fantozzi S, Viceconti M, Taddei F et al (2006) A new software tool for 3D motion analyses of the musculo-skeletal system. Clin Biomech 21:870–879

Martin RB, Burr DR, Sharkey NA (1998) Skeletal tissue mechanics. Springer, New York

Martínez-Reina J, García-Aznar JM, Domínguez J, Doblaré M (2009) A bone remodelling model including the directional activity of BMUs. Biomech Model Mechanobiol 8:111–127

McNamara LM, Prendergast JP (2007) Bone remodeling algorithms incorporating both strain and microdamage stimuli. J Biomech 40(6):1381–1391

McNamara L, Vander Linden J, Weinans H, Prendergast P (2006) Stress-concentrating effect of resorption lacunae in trabecular bone. J Biomech 39(4):734–741

Mullender MG, Huiskes R (1995) Proposal for the regulatory mechanism of Wolff's law. J Orthop Res 13(4):503–512

O'Brien FJ, Taylor D, Clive Lee T (2003) Microcrack accumulation at different intervals during fatigue testing of compact bone. J Biomech 36:973–980

Rafiq MY, Bugmann G, Easterbrook DJ (2001) Neural network design for engineering applications. Comput Struct 79(17):1541–1552

Rho JY, Kuhn-Spearing L, Zioupos P (1998) Mechanical properties and the hierarchical structure of bone. Med Eng Phys 20:92–102

Sansalone V, Lemaire T, Naili S (2007) Multiscale modelling of mechanical properties of bone: study at the fibrillar scale. C R Mec 335(8):436–442

Stulpner MA, Reddy BD, Starke GR, Spirakist A (1997) A three-dimensional finite analysis of adaptive remodelling in the proximal femur. J Biomech 30(10):1063–1066

Taylor M, Cotton J, Zioupos P (2002) Finite element simulation of the fatigue behaviour of cancellous bone. Meccanica 37:419–429

Topping BHV, Bahreininejad A (1992) Neural computing for structural mechanics. Saxe Coburg, UK

Tovar A (2004) Bone remodeling as a hybrid cellular automaton optimisation process. PhD dissertation, University of Notre Dame, Indiana

Unger JF, Konke C (2008) Coupling of scales in multiscale simulation using neural networks. Comput Struct 86(21–22):1994–2003

Viceconti M, Taddei F, Petrone M, Galizia S, Van Sint Jan S, Clapworthy GJ (2006) Towards the virtual physiological human: the living human project. In: Middleton J (ed) 7th International symposium on computer methods in biomechanics and biomedical engineering (CMBBE2006). FIRST Numerics Ltd, Antibes

Viceconti M, Zannoni C, Testi D, Petrone M, Perticoni S, Quadrani P et al (2007) The multimode application framework: a rapid application development tool for computer aided medicine. Comput Meth Prog Biomed 85:138–151

Viceconti M, Taddei F, Jan SVS, Leardini A, Cristofolini A, Stea S, Baruffaldi F, Baleani M (2008) Multiscale modelling of the skeleton for the prediction of the risk of fracture. Clin Biomech 23:845–852

Weiner S, Traub W (1992) Bone structure: from ångstroms to microns. FASEB J 6:879–885

Yoo A, Jasiuk I (2006) Couple-stress moduli of a trabecular bone idealized as a 3D periodic cellular network. J Biomech 39:2241–2252